6th International Conference on Advances in Experimental Structural Engineering
11th International Workshop on Advanced Smart Materials and Smart Structures Technology
August 1-2, 2015, University of Illinois, Urbana-Champaign, United States

Experimental Study and Numerical Simulation on Steel Plate Girders With Deep Section

Y.Y. Zhu[1], J.C. Zhao[2]

1 *Ph.D. Student, Dept. of Civil Engineering, Shanghai Jiao Tong University, Shanghai, China.*
E-mail: cloudybaby@sjtu.edu.cn
2 *Professor, Dept. of Civil Engineering, Shanghai Jiao Tong University, Shanghai, China.*
E-mail: jczhao@sjtu.edu.cn

ABSTRACT
In heavy power plants, steel plate girders are used to suspend the tower-type boilers. Generally, the section of these girders is in a mega size and hence is made of two parts combined by high strength bolts to meet the needs of load carrying and transportation, and the span-depth ratio of these girders are usually less than 6. Thus their mechanical properties are different from normal fabricated girders, the effects of shear deformation can not be neglected. Tests of eight plate girders with deep section, four of which are composite beams, are presented and investigated. A nonlinear finite element analysis is carried out considering the effects of plasticity, residual stress, and geometrical imperfections. The numerical model is verified by experimental results. The distribution of plane stress and shear strain on cross section subjected to interaction of bending moment and high shear force are presented and discussed. The results are compared against traditional theories, to preliminarily reveal the mechanical properties of deep section plate girders. A few suggestions for design process are given.

KEYWORDS: *Plate girders, Experimental tests, Numerical model, Plane stress, Shear deformation*

1. INTRODUCTION

The span of the steel plate girders used in heavy power plants may exceed 40m and the depth of sections can reach 8~10m. Such deep sections are not common in ordinary engineering structures. The mechanical properties of these girders are different in some way, because of their low span-depth ratio and combined sections. Thus the effects of shear deformation can not be neglected. In the experimental process of this research, it is proved that in some cases the effects of shear may be the major factors leading to damage.

Section classification is one of the key points of ANSI/AISC 360-10 [1] and other relevant design codes and standards, which use similar provisions with slightly different limit ratios of width to thickness. In majority of codes, local and global buckling or instability modes are considered separately, leading to the consideration of the cross-section rather than the member. Following the notation of AISC provisions of section classification, it must be ascertained whether local buckling of a single plate is reached before elastic limit (slender); between the elastic and plastic limit (non-compact); or after the plastic limit (compact). Chinese design code for steel structures (GB 50017) [2] also use this strategy to classify cross sections into three groups. Furthermore, the shear buckling is generally not included in the classification procedure, i.e. I-girders retain their class if they are bearing shear force or not. Thus the selection of the analysis procedure should be examined especially for I-girders with high shear ratio where the shear force is greater than half the plastic shear resistance, such as the specimens in this research. And in order to improve the design process and reduce the steel quantity, a classification of I-girders considering both the effects of local interaction and member slenderness is needed.

Recently, studies on limiting width-to-thickness ratios were made on I-girders composed of high strength steel by Earls [3]. It was observed that a decoupling of local and lateral-torsional buckling phenomena is not possible. Kemp [4] proposed a model to account for the interaction between local (including flange and web) and lateral-torsional buckling. Kemp [5] analyzed test results and found out the existence of a much better relationship between rotation capacity and generalized slenderness, if the latter included the slenderness of both local buckling and lateral-torsional buckling. Shokouhian M. [6] proposes a classification of flexural members based on rotation capacity at the member level for the latest version of the Chinese steel design code which takes into account interaction between local and local–overall buckling modes. But the members studied in this

research were only composed to pure bending, and support from testing results were lacking. Cheng Xin [7-9] presented an experimental study of H-section steel beam–columns with large width-to-thickness ratios subjected to combined forces. Conclusion was made that the web–flange interaction is one of the significant features that influence cross-sectional behavior but have received little consideration. The necessity for current specifications to improve those rules has been highlighted. However, there are few corresponding numerical studies in existing literatures, and more experimental investigations for I-girders with high shear ratio were in need.

Another key point in design process is the strength calculation. The steel plate girders we studied are commonly used to support vertical loads from large facilities. They are usually composed of compact flanges, non-compact or slender webs. In these cases web panels are subjected to combination of shear and bending, while the shear force is greater than half the plastic shear resistance. Basler [10] assumed that shear is carried only by the web, the maximum shear resistance is reached when the tension field in the web is fully utilized. Further design models were based on Basler's assumption with different modifications on shear resistance of the web plate and the interaction model. For each of the methods the ultimate shear resistance is defined with modified collapse mechanism. The interaction of bending moment and shear load is defined with either linear expression or quadratic expression. The M–V interaction formula given in Chinese design code [2] is in the same pattern with Eurocode 3 [11]. The method is based on the calculation of the effective cross-section characteristics, and the shear resistance is derived from a tension field model in the web.

Tests of four I-section and four composite section plate girders are presented and investigated. Experimentally verified nonlinear finite element modeling techniques were employed herein to conduct further parametric studies on structural members of this type.

2. EXPERIMENTAL PROGRAM

2.1. Test Specimen

Four I-section (labeled “G”) and four composite section (combined by high strength bolts, labeled “D”) beams welded from Q235 and Q345 flame-cut plates were comprised in this test program, as summarized in Tables 1 and 2 where the sectional geometric parameters are illustrated in Fig. 1 and 2. All sections were designed as compact flanges and non-compact webs, to meet the real conditions. In addition, the section dimensions were determined not so large because of the scale limit of the test equipment. For welded I-section beams, web of 8mm thick and flange of 16mm plates are used, with fillet welds size 8mm. The unbraced lengths (L_b) and distance between transverse stiffeners are also given in Tables 1 and 2. Besides, the section and member classification according to ANSI/AISC 360-10 are also summarized in these two tables.

Two standard tension coupons were prepared and tested to determine the mechanical properties of steels for each thickness of the original steel plates from which the column specimens were manufactured. Two strain gauges were equipped on both sides at the mid-length of coupons to measure the longitudinal strains for accurate determination of Young's Modulus, and an extensometer was attached on one side to obtain the strains after the failure of the strain gauges.

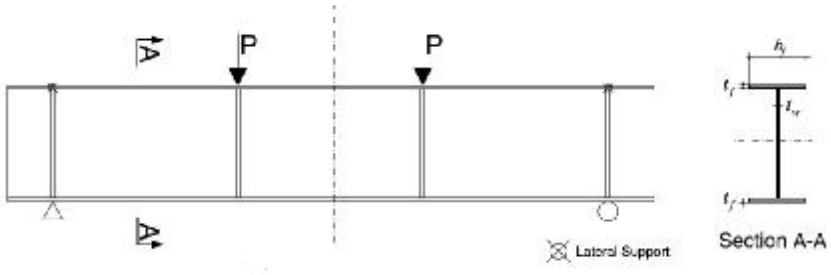

Figure 2.1 Sketch of I-section plate girders (not to scale)

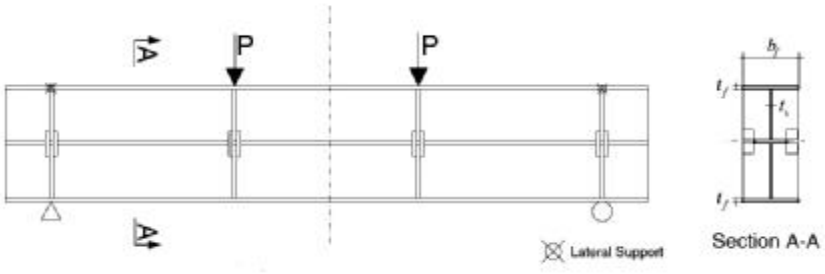

Figure 2.2 Sketch of composite section plate girders (not to scale)

Table 2.1 Size and member classification of I-section beams (unit: mm; material: Q235)

Label	Section ($h\times b\times t_w\times t_f$)	Unbraced length (L_b)	Span-to-depth ratio (L_b/h)	distance between transverse stiffeners	member classification
G1	600×180×8×16	2700	4.5	900 (1.5h)	inelastic lateral-torsional buckling
G2	600×180×8×16	3600	6	1200 (2h)	
G3	860×180×8×16	2700	3.14	900 (1.05h)	
G4	860×180×8×16	3600	4.19	600 (0.7h)	

Table 2.2 Size of composite section beams (unit: mm)

Label	Upper part ($h\times b\times t_w\times t_f$)	Lower part ($h\times b\times t_w\times t_f$)	Unbraced length (L_b)	Span-to-depth ratio ($L_b/2h$)	Material
D1	300×180×8×16	300×180×8×16	3600	6	Q235
D2	430×180×8×16	430×180×8×16	3600	4.19	
D3	300×180×8×16	300×180×6×12	3600	6	upper part Q235 lower part Q345
D4	430×180×8×16	430×180×6×12	3600	4.19	

2.2. Test Configurations

As illustrated in Fig. 1 and 2, all specimens were subject to concentrated load through the 10000kN hydraulic actuator WAW-1000J. Strains and deflections were continuously measured. The mid-span deflection of the girder was measured by displacement transducers, to monitor the overall performance of the girders and for verification of the numerical models. Strain gauges were set along the mid-span cross section of the girders, subjected to constant bending moment. To monitor the local buckling and yielding of web plate, strain rosettes were set in the web grid under combined forces, and distributed in four cross sections. The test configuration is shown in Fig. 3 and 4.

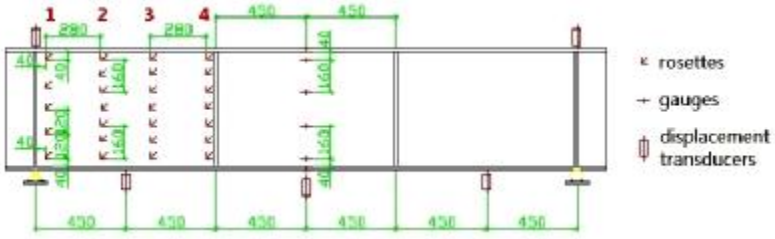

Figure 2.3 Test configurations of I-section plate girders (G1)

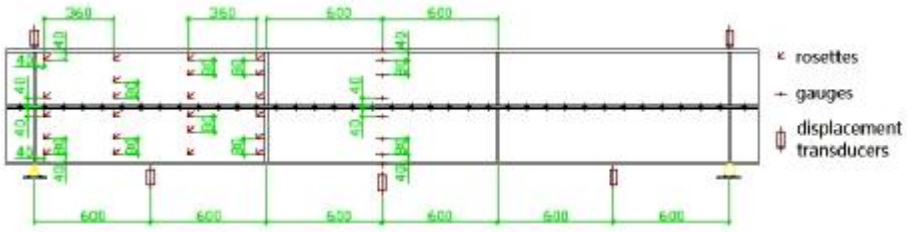

Figure 2.4 Test configurations of composite section plate girders (D1)

3. TEST RESULTS AND ANALYSIS

3.1. Material Mechanical Property

The stress–strain curves for each kind of plates are obtained from tension coupon tests. The stress (σ) was the applied load divided by the initial area, and the strain (ε) was the average of readings from two strain gauges. The primary mechanical properties obtained from the tension coupon test are summarized in Table 3. The experimental data shown were the average results from two coupons for each thickness plate, and would be adopted in finite element models.

Table 3.3 Primary mechanical properties of the plates

Material	Thickness (mm)	Ultimate stress (MPa)	Young's Modulus (MPa)	Yield strength (MPa)
Q235	8	450	211602.15	285
Q235	16	420	205010.79	245
Q345	6	565	202908.60	400
Q345	12	480	206733.89	325

3.2. Behavior of the Tested Girders

Failure modes of the tested specimens can be divided into three types, to be the basis of a classification method. Two more types were proved to be existing by parametric study afterwards. Typical characteristics of these five types are listed in Table 4. In addition, when the capacity in load-deflection curve of a girder falls below 70% of its peak value, the specimen can be judged fail.

Table 3.4 Typical characteristics of failure modes

Type	Local buckling	Max normal strain (bending grid)	Lateral-torsional buckling	Specimen(s)
Ⅰ*	occur	$<\varepsilon_y$	not occur	G3
Ⅱ*		$>\varepsilon_y$	not occur	G1
Ⅲ			occur	proved to be existing
Ⅳ	not occur		not occur	
Ⅵ			occur	G2, G4 and D1-4

This kind of classification is based on three characteristics: the local buckling of web panel subjected to shear; whether the maximum normal strain measured by strain gauges exceeds the yield strain ε_y; the lateral-torsional buckling of whole girder. Examples of local buckling and lateral-torsional buckling are shown in Fig. 5 and 6. Fig. 7 shows the failure pattern of composite beams. Detailed results and data will be mentioned in following discussions. Characteristics of type Ⅰ and Ⅱ (highlighted with "*" in Table 4) prove that in some cases the effects of shear may be the major factors leading to damage instead of bending.

Figure 3.5 Example of local buckling (G3)

Figure 3.6 Example of lateral-torsional buckling (G4)

Figure 3.7 Composite beam failure (D1 for example)

4. NUMERICAL SIMULATIONS

4.1. Numerical Model

A nonlinear finite element analysis was carried out using commercial FEA software ANSYS 14.5. The combined effects of plasticity, residual stress, and geometrical imperfections are considered, to simulate the experimental phenomena. Modeling strategy proposed by Zhang L. and Tong G. S. [12] is adopted here, as fewer assumptions are adopted in shell theory than beam theory, to get more precise results. Element type SHELL 181 is used for flanges and webs, which is a kind of four node element with six degrees of freedom each node, and applicable to nonlinear analysis with large deformation. Two concentrated loads located at L/3 along the span length of simply-supported I-shaped beams assembly are imposed. The material properties of steel plates were modeled with a 2-linear curve, i.e. "Bilinear Isotropic Plasticity" to describe the constitutive models.

The strategy of seeding the finite element mesh with an initial displacement field is employed in this study. In this technique, the idealized model is subjected to an eigenvalue buckling analysis from which an approximation to the first buckling mode of the girder is obtained. The displacement field associated with this lowest mode is attached to the idealized model afterwards as a seed imperfection for use in the incremental nonlinear analysis. The maximum initial displacement of this seed imperfection is considered in two types, local and overall geometrical imperfections according to the Chinese code for acceptance of construction quality of steel structures GB50205 [13]. It shows that the existing of residual stress will affect the interaction between local buckling and global failure. Self-balance parabolic model is adopted to describe it, which was proved to be more realistic [14]. Quadratic distribution is taken for flanges and four times distribution for webs.

4.2. Comparative Results and Model Verification

4.2.1. Capacity and failure mode

A typical loading-vertical displacement curve of specimen G1 was shown in Fig. 8, in which the ordinate was the total loading (2P in Fig. 1) applied and the abscissa was the horizontal displacement at the mid-length,

obtained from readings of displacement transducers (Fig. 3). It can be seen in Fig. 8 that the two curves in this figure were in good agreement. The error of capacity between simulations and tests were kept within 5% for all 8 specimens. Typical failure modes are shown in Fig. 9, meeting the experimental results as well. The finite element model is verified, and can be used for numerical analysis.

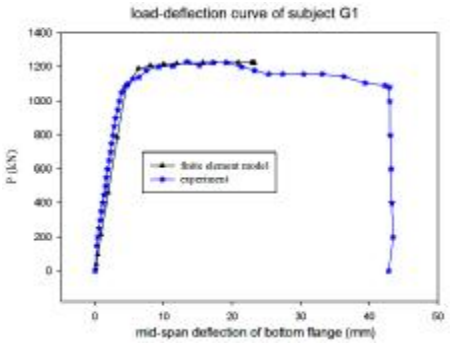

Figure 4.8 Typical loading-vertical displacement curve (G1).

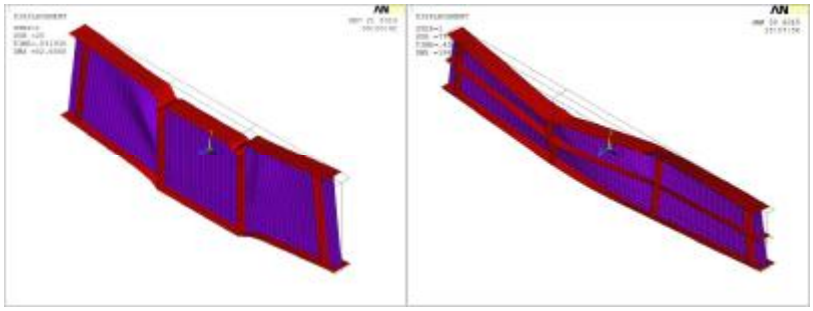

Figure 4.9 Typical failure modes (G3 for local and D1 for global failure).

4.2.2. Deformation

The characteristic deformation in the member classification research is the maximum normal strain ε_u coursed by bending. It must be ascertained whether ε_u exceeds the yield strain ε_y or not, as mentioned above. Fig. 10 and 11 shows the maximum normal strain curve of G1 and G3 respectively, to help understand that.

According to the material mechanical properties, the yield strain ε_y of flange plates of G1 and G3 is about 1200με. It can be seen in Fig.10 that the maximum normal strain ε_u of both flanges exceeds ε_y, and the load-strain curves begin to develop nonlinearly. On the contrary, Fig.11 shows that the ε_u of G3 is close to ε_y but did not exceed it. And it can be easily figure out that the strain ratio $\varepsilon_u/\varepsilon_y$ will get smaller with the decreasing span-to depth ratio of the member. In addition, the load-strain curve of upper and bottom flange of G3 (Fig.11) develop in different trends because the real condition was not idealized pure bending for short and deep specimens, and the local buckling caused stress redistribution between different parts of the member. And signs of material yielding still exist due to the imperfection of material and the deviation of installation and loading.

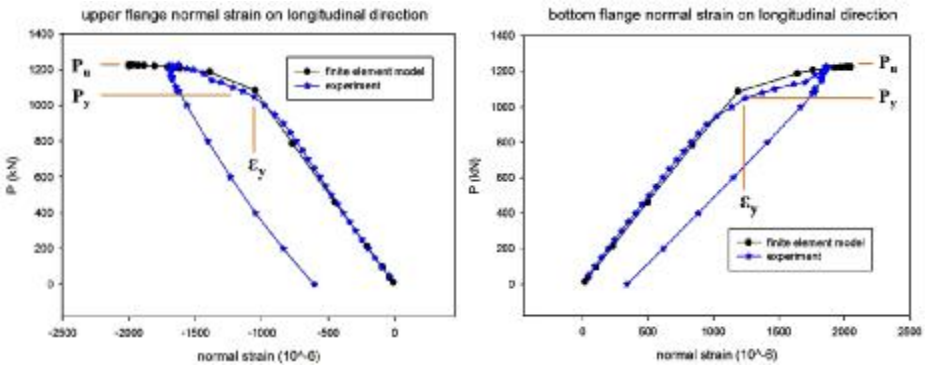

Figure 4.10 The maximum normal strain curve of G1 ($\varepsilon_u > \varepsilon_y$).

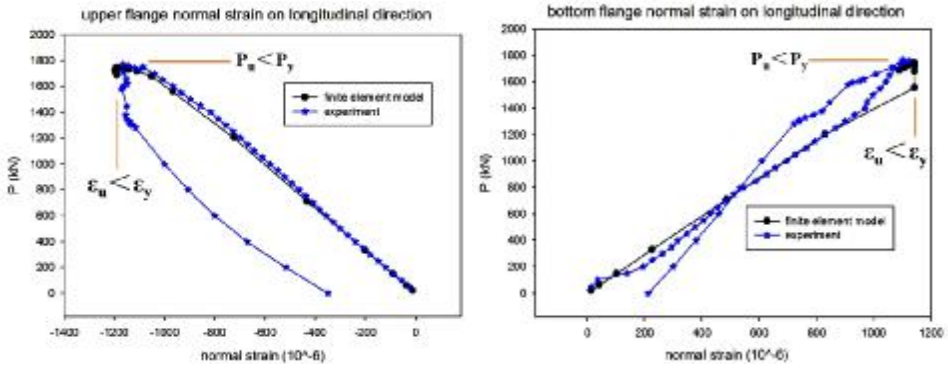

Figure 4.11 The maximum normal strain curve of G3 ($\varepsilon_u < \varepsilon_y$).

5. DISCUSSION ON DESIGN METHODS

The section classification of the I-section specimens are compact flanges and non-compact webs, and member classification are inelastic lateral-torsional buckling, according to ANSI/AISC 360-10, as well as GB 50017. But for specimen G1, the elastic limit was reached in bending grid ($\varepsilon_u > \varepsilon_y$) while global inelastic failure did not occur. For specimen G3, even the elastic limit was not reached ($\varepsilon_u < \varepsilon_y$). It can be seen that local buckling were reached ahead of the estimation of code provisions, because the span-to-depth ratio of these two specimens are small, and shear becomes the dominating load. But, for specimen G4 with similar span-to-depth ratio, extra transverse stiffeners were set in the middle section of shear grids, local buckling has been successfully prevented. Thus, a supplement of code terminology of section classification for I-girders with high shear ratio where the span-to-depth ratio is below 6 is needed, and the effects of transverse stiffeners (distance between transverse stiffeners) should be taken into account. The classification method mentioned above can be promoted.

In design process, Basler's assumption (shear is carried only by the web) is taken and the shear strain is calculated according to the plane cross-section assumption. It can lead to either two conclusions that the shear strain is constant along the section, or the maximum shear strain lies in the neutral axis of the cross section. But tests and numerical analyses show that the maximum shear strain lies above the neutral axis in sections close to the concentrated forces, and below the neutral axis in sections close to the supported ends. Such phenomenon is caused by the distribution of transverse normal stress, which is also neglected by code provisions and traditional beam theories. Such strain field can be derived through theory of elasticity [15]. Detailed strain data and derivation process will be performed later. Fig. 12 shows the typical distribution of shear strain in web plane and the brief explanation of tension field in this case.

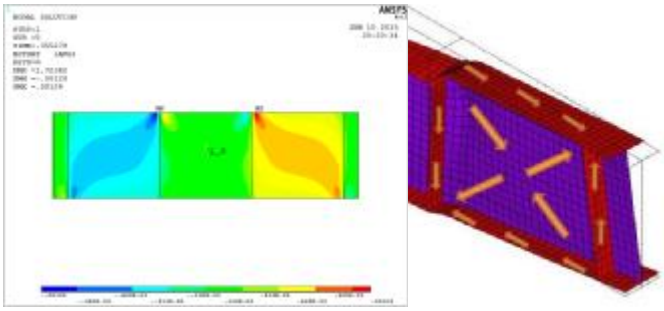

Figure 5.12 Typical distribution of shear strain and distribution of tension field (G3).

6. CONCLUSIONS

The buckling behavior of 4 I-section beams and 4 composite section beams fabricated from flame-cut plates were investigated. Based on the test results, the buckling types of this kind of member were clarified in detail, and a FEM model was established and verified based on the experimental results. The results were briefly compared with existing design methods. Based on these work, the following conclusions were made:

1) The verified FEM in this investigation could accurately estimate the capacity and failure of plate girders, in which the effects of initial geometric imperfections and residual stresses were included.
2) A supplement of code terminology of section classification for I-girders with high shear ratio is needed. The effects of the web–flange interaction of sections, the span-to-depth ratio of members, and the reinforcement of transverse stiffeners should be taken into account. The strategy for classification presented in this research can be further studied and promoted to practical level.
3) Effects of shear plays important role in I-section girders where span-to-depth ratios are less than 6. The actual distribution of shear deformation on cross section should be derived through theory of elasticity, and corresponding design methods for local buckling should be modified.

Both the experimental investigation and modeling procedure could provide valuable information for future beam researches and engineering application.

AKCNOWLEDGEMENT
The authors gratefully acknowledge sponsors of this research: National Science Foundation of China (No. 51278296). Thanks are also extended to the Laboratory of Civil Engineering of Shanghai Jiao Tong University for the test equipment and conditions provided.

REFERENCES

1. ANSI, A. (2010). AISC 360-10: Specification for Structural Steel Buildings. American Institute of Steel Construction Inc, Chicago, IL.
2. GB 50017-2003. (2003). Code for design of steel structures. Beijing, China: National Standard of the People's Republic of China.
3. Earls, C. J. (1999). On the inelastic failure of high strength steel i-shaped beams. Journal of Constructional Steel Research, 49(98), 1–24.
4. Kemp AR (1986). Factors affecting the rotation capacity of plastically designed members. Struct Eng , 64B(2): 2835.
5. Kemp, A. R. (2014). Inelastic local and lateral buckling in design codes. Journal of Structural Engineering, 122(4), 374-382.
6. Shokouhian, M., & Shi, Y. (2014). Classification of i-section flexural members based on member ductility. Journal of Constructional Steel Research, 95(3), 198-210.
7. Cheng, X., Chen, Y., & Nethercot, D. A. (2013). Experimental study on H-shaped steel beam-columns with large width-thickness ratios under cyclic bending about weak-axis. Engineering Structures, 49, 264-274.
8. Chen, Y., Cheng, X., & Nethercot, D. A. (2013). An overview study on cross-section classification of steel H-sections. Journal of Constructional Steel Research, 80, 386-393.
9. Cheng, X., Chen, Y., & Pan, L. (2013). Experimental study on steel beam–columns composed of slender H-sections under cyclic bending. Journal of Constructional Steel Research, 88, 279-288.
10. Basler K (1961). Strength of plate girders under combined bending and shear. J Struct Div ASCE, 87.
11. CEN. (2006). EN 1993-1-5: Eurocode 3: Design of Steel Structures. Part 1-5: plated structural elements. Brussels: European Committee for Standardisation.
12. Zhang, L. and Tong, G. S. (2008). Lateral buckling of web-tapered I-beams: A new theory. Journal of Constructional Steel Research, 64(12), 1379-1393.
13. GB50205 (2001). Code for acceptance of construction quality of steel structures. Beijing, China: National Standard of the People's Republic of China.
14. Gardner, L., & Cruise, R. B. (2009). Modeling of residual stresses in structural stainless steel sections. Journal of Structural Engineering, 135(1), 42-53.
15. Timoshenko, S. P., & Goodier, J. N. (2014). Theory of elasticity. International Journal of Bulk Solids Storage in Silos, 1(4).